Soft Matter

Viability of Lactobacillus rhamnosus GG microencapsulated in alginate/chitosan hydrogel particles during storage and simulated gastrointestinal digestion: Role of chitosan molecular weight

Journal:	*Soft Matter*
Manuscript ID	SM-ART-12-2019-002387.R1
Article Type:	Paper
Date Submitted by the Author:	10-Jan-2020
Complete List of Authors:	Qi, Xiaoxi; North Dakota State University Simsek, S.; North Dakota State University, Plant Sciences ohm, Jae-Bom; United States Department of Agriculture, District of Columbia (USDA); United States Department of Agriculture, District of Columbia (USDA) Chen, Bingcan; North Dakota State University, Plant Sciences Rao, Jiajia; North Dakota State University, Plant Sciences

Viability of *Lactobacillus rhamnosus* GG microencapsulated in alginate/chitosan hydrogel particles during storage and simulated gastrointestinal digestion: Role of chitosan molecular weight

Xiaoxi Qi[1], Senay Simsek[1], Jae–Bom Ohm[2], Bingcan Chen[1], Jiajia Rao[1*]

1. Food Ingredients and Biopolymers Laboratory, Department of Plant Sciences, North Dakota State University, Fargo, ND 58108 United States

2. Edward T. Schafer Agricultural Research Center, Cereal Crops Research Unit, Hard Spring and Durum Wheat Quality Lab, USDA–ARS, Fargo, North Dakota 58108, United States

Submission Journal: Soft Matter

Revision submitted on Jan. 2020

*To whom correspondence should be addressed. Tel: 1 (701) 231-6277. Fax: 1 (701) 231-7723. E-mail: jiajia.rao@ndsu.edu.

Abstract

Sodium alginate hydrogel particles coated with cationic biopolymers has shown to be one of the promising means for probiotics encapsulation and protection. In this study, we aimed to systematically explore the effect of molecular weight of chitosan coating on the functional performance of sodium alginate hydrogel particles in improving viability of *Lactobacillus rhamonsus* GG (LGG). We first electrostatically deposited three different molecular weight of chitosan, i.e., chitosan oligosaccharide (COS), low molecular weight chitosan (LMW–chitosan) and medium molecular weight chitosan (MMW–chitosan) on sodium alginate hydrogel particles. Both SEM and FTIR results indicated that chitosan was successfully deposited to the surface of the hydrogel particles. We then evaluated the effect of chitosan MW on the viability of LGG encapsulated in the hydrogels during long-term storage and under simulated gastrointestinal digestion. Among them, the hydrogel particles coated with COS prevented the viability loss of LLG during long-term storage under different temperature (4, 25 and 37 °C). However, we did not found any improvement on the viability of encapsulated LGG by all three chitosan coatings in simulated digestion.

Keywords: Chitosan oligosaccharide; low molecular weight of chitosan, medium molecular weight of chitosan, sodium alginate hydrogel, probiotics; *in vitro* digestion.

Introduction

In recent years, a number of studies have proved that probiotics such as *Lactobacillus rhamonsus* GG (LGG) have positive effects on alleviating inflammatory conditions, infectious and immunity system problems in human beings [1, 2]. These findings have triggered the consumers' desire for relevant products which have promoted the application of probiotics in the food industry. To exert the health effects, it is recommended to ingest food with at least 10^6–10^7 colony forming units (CFU)/g viable probiotics [3]. However, most of the probiotics are highly susceptible to all kinds of environmental stresses occurred during processing and storage, or when passing through the human gastrointestinal tract (GI), thus causing the loss their viability and potential health benefits [4]. For example, it was observed that two strains of probiotics, *Lactobacillus acidophilus* and *Bifidobacterium bifidum* lost their viability consistently during refrigerated storage in five commercial yogurts [5]. The considerable loss of probiotics viability was also observed during food manufacturing procedures and improper storage conditions in other probiotics-containing products, such as cheeses [6], fruit juices [7], and chocolate [8]. In terms of human digestion, the loss of the majority or even the entire probiotics were frequently reported in literatures [9, 10]. This is presumably caused by the low gastric pH in conjunction with the presence of bile salt and enzymes in the GI tract [11].

Recently, microencapsulation of probiotic bacterial in food biopolymer matrix using different technologies such as emulsion, coacervation, and extrusion technologies have been explored which achieved various degrees of success on improving the cell viability [12-14]. Among them, cross-linked sodium alginate (ALG) hydrogels have received much of interests because of its good gelling property with nutritional minerals such as Ca^{2+} [15], low cost, non-toxicity, valued GRAS (generally recognized as safe) status and as well simplicity of operation [16, 17].

Nevertheless, previous study also pointed out that the semi-permeable alginate hydrogels were degraded or even collapsed when excess amount of monovalent existed such as Ca^{2+} chelators, and at acidic pH (e.g., pH 3) [18]. In order to overcome the semi-permeability of a single hydrogel system, some attempts have been made to create a multilayer coating of biopolymers on the surface of alginate hydrogel particles by blending alginate with other food biopolymers, such as starch, whey protein, and chitosan through electrostatic deposition at a designated pH [19, 20, 21].

Chitosan is a linear cationic polysaccharide composed of randomly distributed β-(1→4)-linked D-glucosamine and N-acetyl-D-glucosamine residues [22]. Under acidic conditions, the positively charged amine groups (pKa~6.5) in chitosan enables the electrostatic interaction between chitosan and other anionic biopolymers including sodium alginate [22]. Based on the molecular weight (MW), chitosan is divided into four types: chitosan oligosaccharide (COS), low–molecular–weight (LMW) chitosan, medium–molecular–weight (MMW) chitosan, and high–molecular–weight (HMW) chitosan. As different types of chitosan contain variable amount of surface charge, one would expect the physicochemical properties of chitosan coatings on alginate hydrogel particles could be influenced by their different molecular weight. In addition, different types of chitosan exhibit unique mechanical properties, e.g., LMW- chitosan has higher textural strength compared to MMW-chitosan [23]. Thus, the MW of chitosan may also influence the fate of alginate encapsulated probiotics, such as cell release during storage stability and/or in GI tract. Nonetheless the effect of molecular weight of chitosan coatings on the survivability of the encapsulated probiotics in sodium alginate hydrogel has not been fully elucidated to date. Hence, the objective of this research is to investigate how chitosan with different molecular weight behaves differently on modulating survivability of LGG (a widely studied and used probiotics) encapsulated in chitosan coated sodium alginate hydrogels during storage at different

temperature (4 °C and 25 °C) as well as in simulated GI tract. In addition, the physiochemical properties of chitosan coated sodium alginate hydrogels including particle size, surface charge, texture profile, and microstructural morphology were also investigated to determine the possible mechanisms by which physical properties of hydrogels impact the viability of encapsulated probiotics.

Materials and methods

Materials

Sodium alginate (ALG), LMW-chitosan (50–190 kDa, degree of deacetylation: 75~85%), MMW-chitosan (190–310 kDa, degree of deacetylation: 75~85%), sodium citrate pepsin, bile extract and pancreatin were purchased from Sigma-Aldrich Chemical Co., Ltd, (St. Louis, MO, USA). Chitosan oligosaccharide (COS, 5 kDa, degree of deacetylation: > 90%) was purchased from Tokyo Chemical Industry Co., Ltd, (Tokyo, Japan). Ultrapure water was obtained from a Barnstead GenPure Pro water purification system (18.2 MΩ·cm, Thermo Fisher Scientific Inc., USA).

Strains and culture conditions

Lactobacillus rhamnosus GG (LGG) ATCC 53103 was purchased from the American Type Culture Collection (ATCC) (Manassas, VA, USA). The LGG was cultured in MRS broth (Sigma-Aldrich Chemical Co., Ltd, St. Louis, MO, USA) or MRS agar (Beckton Dickinson and Company, Sparks, MD, USA) at 37 °C under anaerobic condition for 24 h. The bacterial cells in broth were harvested by centrifugation (Sorvall™ biofuge primo centrifuge, Thermo Scientific Inc., MA, USA) at 8000 rpm for 15 min at 4 °C and washed twice by ultrapure water. The pellet was resuspended in 0.1% (w/v) peptone solution to obtain a suspension containing approximately 11 log (CFU/ml) cells. For each experiment, cell suspensions were prepared

freshly, which was then dissolved in 1% (w/v) sodium citrate solution and numerated by plating appropriate ten-fold dilutions onto MRS agar after 48 h of incubation at 37 ℃.

Encapsulation of LGG sodium alginate hydrogel particle

LGG was encapsulated in sodium alginate hydrogel particles through an extrusion method described by Trabelsi et al [24] with a slight modification. Briefly, bacterial cell suspension was mixed with 2 % (w/v) ALG solution to achieve an approximate concentration of 10 log (CFU/mL). The mixture was then extruded from a syringe with a 22 gauge needle equipped with a syringe pump (LEGATO® 100 syringe pmp, KD Scientific Inc., MA, USA) at the rate of 4 mL/ min into 100 mL 0.15 M $CaCl_2$ solution with constant stirring. The hydrogel particles were immediately formed by contacting with $CaCl_2$ solution and left in the solution for hardness for 30 min. The hydrogel particles were then harvested using a sieve which was then washed with ultrapure water twice. Approximately loading number of bacterial cells was tested to be 9.4×10^9 per gram beads.

Preparation of chitosan coated hydrogel particles

Bulk chitosan solutions (COS, LMW–chitosan and MMW–chitosan) at a fixed concentration of 0.1% (w/v) were prepared by dissolving 1.0 g of chitosan in 1.0 L acetic buffer (10 mM), and then pH was adjusted to 6 using 1.0 M NaOH. The ζ–potential of each solution was measured by Malvern Zetasizer Nano ZS (Malvern Panalytical Ltd., Worcestershire, UK).

The chitosan coated alginate hydrogel particles were prepared by adding 10.0 g of ALG particles into 90 mL of freshly prepared chitosan solutions (0.1 %, w/v). ALG particles in the absence of chitosan were used as a control. All samples were stirred at 300 rpm for 45 min, and the particles were harvested and washed with ultrapure water prior to use.

Diameter of hydrogel particles

The shapes of 30 randomly selected particles of each treatment were captured by an Olympus SHE dissecting light microscope (Olympus Optical Co., Ltd., Japan) with moticam 5 digital camera (Motic Instruments Inc., Richmond, BC, Canada) and the average diameter was analyzed by the Motic Images Plus 3.0 software.

Textural properties of hydrogel particles

Method used to measure the textural properties of hydrogel particles was adapted from Bourne [25] by a Stable Micro Systems Texturometer model TA–XT2i (Texture Technologies Corp., White Plains, NY, USA) equipped with a 5 kg load cell. A 35 mm diameter cylindrical steel probe was applied on 30 g of particles harvested for each treatment in a compression mode at a constant crosshead velocity of 2 mm/s. The rupture force measurements were carried out on the entire particles form each treatment at a velocity of 5 mm/s in a distance mode. The peak force was measured in newtons. The automatic detection of the contact between the probe with the particles was carried out with a contact force of 0.005 N. Textural properties of hydrogel particles including hardness, springiness, cohesiveness, and resilience were obtained from the Texture Expert Software for Windows Version 3.2 installed in the equipment [26].

Structural properties of hydrogel particles

Scanning electron microscopy (SEM) (JEOL Mod. JSM-6490LV, Jeol, Peabody, MA, USA) was applied to evaluate the surface morphology and the microstructure of hydrogel particles. Briefly, the hydrogel particles were frozen in liquid nitrogen to prevent the particle shrink during freeze-drying process and to maintain the original structure of the particles, followed by lyophilization for 24 h (Lyophilizer, SP scientific, Gardiner, New York). The dried particles were cut in half and attached to adhesive carbon tab on cylindrical aluminum mount, and then the sample was

coated with gold (Cressington 108auto, Ted Pella Inc., CA, USA) and examined at different magnifications with an accelerating voltage of 15 kV.

Fourier transform infrared spectroscopy (FTIR)

FTIR spectra of all dried hydrogel particles and control powders (ALG, chitosan) were obtained by a Varian FTIR spectrophotometer (California, USA) according to previously published paper without any modification [27].

Survival of the encapsulated cells in simulated gastrointestinal condition

One gram of freshly prepared hydrogel particles was added in a tube with 9 mL of simulated gastric fluid (SGF) (0.08 M HCl containing 0.2 % w/w NaCl, pH 2.0) with 0.3 % (w/v) pepsin and incubated in a shaking water bath (VWR shaking water bath, VWR International, LLC, PA, USA) at 37 °C, 150 rpm for 30, 60, 90, 120 min. After incubation, the particles were filtered and rinsed by ultrapure water twice and then added into 1 % (w/v) sodium citrate solution to release the bacterial cells from the hydrogel particle. The viable cells after SGF were counted by plating the appropriate dilutions onto the MRS agar and incubating under 37 °C for 48 h.

To investigate the survival of LGG in simulated intestinal fluid (SIF), 1.0 g of hydrogel particles was added into a tube with 9 mL SIF (0.05M KH_2PO_4, pH 7.4) containing 1.0 % (w/v) bile salt and 1.0 % (w/v) pancreatin [28, 29]. The tubes were incubated at 37 °C, 150 rpm for 150 min. After incubation in SIF, the viable cells were counted by above-mentioned method.

Storage property measurement

For storage stability test, freshly prepared hydrogel particles were stored in sterilized 0.1 % peptone at three different temperatures, i.e, 4 °C, 25 °C and 37 °C. The viability of encapsulated LGG during storage was measured by the same method described above.

Statistical analysis

The characterization of physical properties of freeze-dried hydrogel particles were performed at least twice. The viability of cell measurement was performed at least four time using freshly prepared samples and values were expressed as means ± SD. Significant differences between means ($p < 0.05$) were conducted by one-way analysis of variance (ANOVA) (Version 9.3, SAS Institute Inc., NC, USA).

Results and Discussions

Chitosan solution and hydrogel properties

ζ–potential of chitosan solutions

As mentioned earlier, chitosan is a product of deacetylation and degradation of chitin. As the increase of degree of deacetylation (DD%), more amine groups in chitosan are exposed to the environment. This is important for the electrostatic attraction between chitosan and ALG, since the amine groups will be protonated which confers net positive charge while ALG brings negative charge under acidic conditions. The DD% of COS is greater than 90% and sometimes can even reach up to 99.9% according to the literatures [30-32]. Due to the varied DD%, we expected that three kinds of chitosan used in the current study should have different electrostatic binding potentials to the surface of sodium alginate hydrogel particles, which can be partially presented by the ζ–potential of the chitosan solutions.

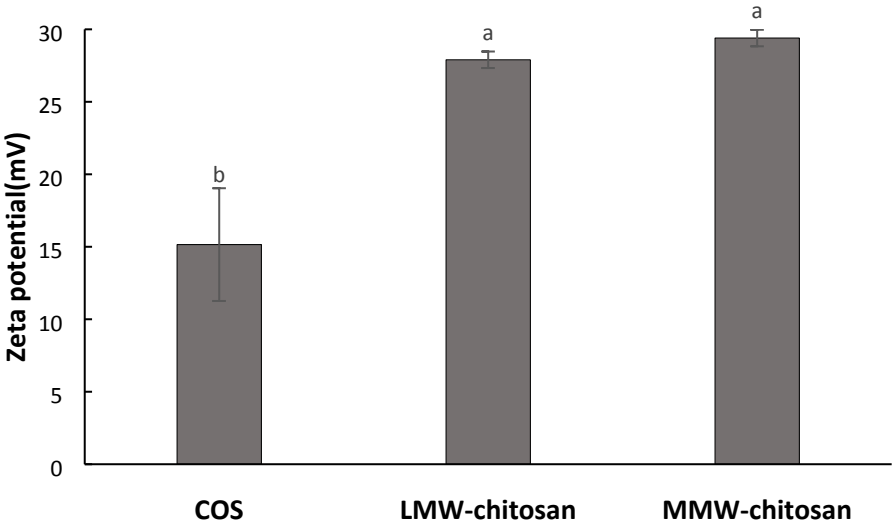

Fig. 1. ζ–potential of 0.1% (w/v) chitosan oligosaccharides (COS), low-molecular-weight chitosan (LMW–chitosan) and medium-molecular-weight chitosan (MMW–chitosan) at pH=6. Different lowercase letters indicate that the means differ significantly ($p < 0.05$).

As shown in **Figure** 1, COS showed an apparently lower ζ–potential compared to LMW–chitosan and MMW–chitosan ($p < 0.05$), while there was no statistically significant difference between the other two at pH 6.0. These results were consistent with other research [33, 34]. The relatively lower ζ–potential of COS could be explained by the destruction of the amine groups caused by the harsh conditions, such as acid, base, oxidative reductive agents and/or high-energy impact treatments used to achieve the higher DD% and smaller molecular weight of COS during the producing process [35]. However, the ζ–potential of chitosan solution is not the only and ample indicator of the interaction between chitosan and sodium alginate particles. The particle size of chitosan also plays a vital role in chitosan coated hydrogel. The bigger the particle size of chitosan is, the stronger steric hindrance there will be in the system. Therefore, the SEM images of the hydrogel particles in the presence and absence of chitosan coatings were taken to elucidate how the particle size of chitosan molecule influenced their electrostatic interaction with ALG and the corresponding morphology of hydrogels in the following part.

Hydrogel particles size and morphology

It has been reported the diameter of the hydrogel particle was strongly influenced by extrusion operation parameters such as wall material, needle gauge, needle to calcium chloride solution distance and ionic strength of gelling solution. Among all the factors, needle gauge of syringe used during extrusion predominantly determines the diameter of hydrogel particles [36]. Muthukumarasamy and others [37] reported that alginate hydrogel particles formed from extrusion method with a diameter in 2–4 mm range showed the better protective effect on the probiotic encapsulated in it.

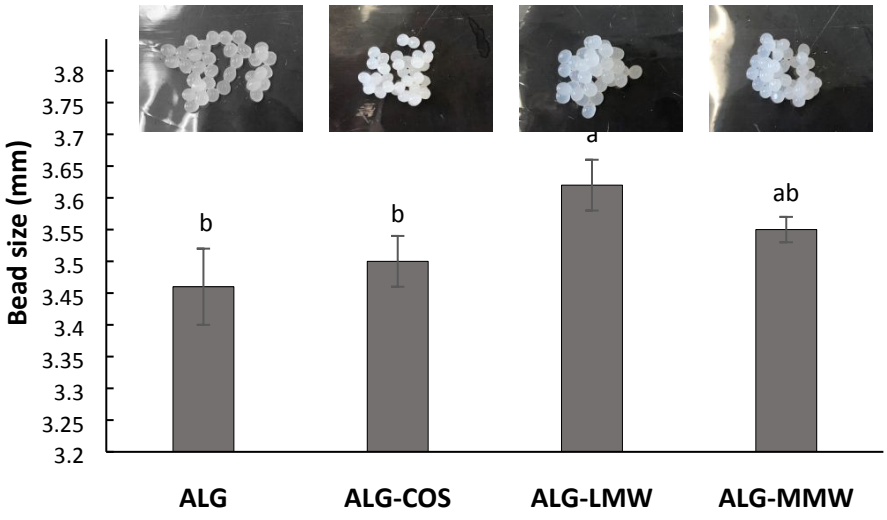

Fig. 2. Diameter of hydrogel particles in the presence and absence of chitosan coating. Picture above the column shows the corresponding morphology of the hydrogel beads. Different lowercase letters indicate that the means differ significantly ($p < 0.05$).

With regarding to the impact of chitosan coating on the size of hydrogel particles, some research found that the addition of chitosan coating had no influence on the size of ALG hydrogel particles [38]. According to the current results (**Figure 2**), coating increased the diameter of ALG hydrogel particles to 3.45 mm which was comparable with other reports [39]. And higher

MW of chitosan exerted greater increment on particle size, which was in a good agreement with earlier studies [40]. These results were supported by the cross-section SEM images (**Figure 3 B-2, C-2, & D-2**) of hydrogel particles in which the external porous surface of sodium alginate hydrogel particles was at least partially covered by chitosan, thus preventing the hydrogel particles from shrinking to a certain level. Among all the chitosan coated ALG hydrogel particles, ALG–COS had the smallest particle size that was comparable with control (ALG). This was also corroborated by SEM image where a thinnest layer with the smoothest surface was observed in ALG–COS particles (**Figure 3 B-3**). Interestingly, ALG–LMW had significant larger ($p < 0.05$) particle size. Presumably, smaller MW of LMW would form less steric hindrance, so a large amount of LMW could be electrostatic deposited on the surface of ALG particle than that of MMW–chitosan. As demonstrated in **Figure 3 D-3**, part of the MMW–chitosan coating was more irregular and partially exfoliated from the hydrogel particle.

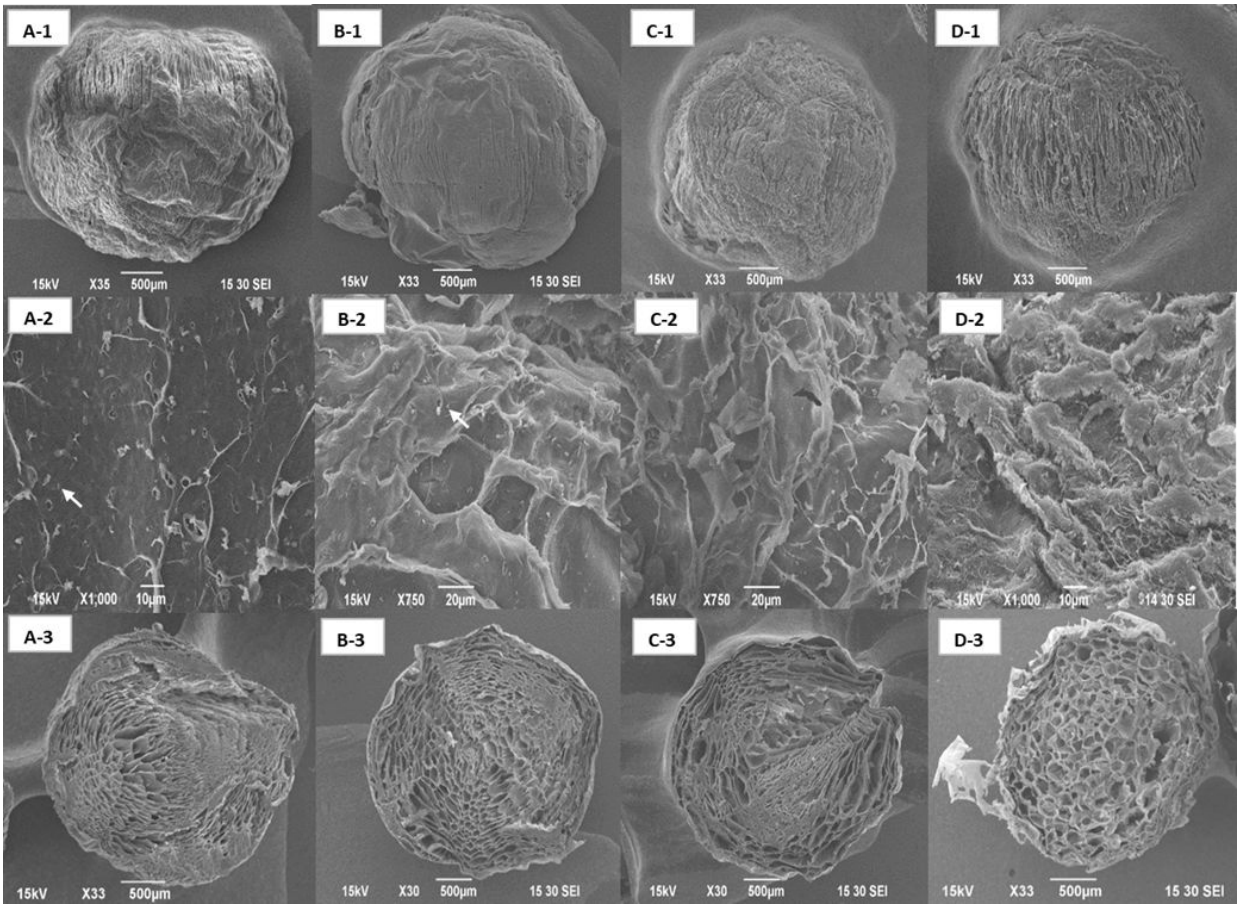

Fig. 3. Morphology of freeze-dried hydrogel particles in the absence and presence of chitosan coating observed by SEM. Sodium alginate hydrogel particles (ALG): (A) in the absence of chitosan; (B) coated with chitosan oligosaccharides (ALG-COS); (C) coated with LMW–chitosan (ALG-LMW); and (D) coated with MMW–chitosan (ALG-MMW). 1 & 2 denotes exterior morphology of hydrogel particles under with two different magnifications; while 3 represents the cross-section view of hydrogel particles. LGG cells under microscopy are highlighted by the arrows in A-2 and B-2. Arrows in D-3 show the protruded chitosan layer.

From the exterior and interior morphology of particles, we also observed that the freeze-dried ALG hydrogel particles produced by extrusion method maintained a spherical or relatively spherical shape, independent of chitosan coating. However, the surface morphology of samples coated with different MW of chitosan was strongly altered as compared to the control. Analyzing the results from a closer perspective as in **Figure 3 A-2, B-2, C-2 & D-2**, ALG particle presented a relative smooth surface, whereas chitosan coating contributed to a more irregular and jagged

surface. The images clearly indicated that the chitosan was successfully deposited onto the external surfaces of the alginate hydrogel particles. Similar appearance of chitosan coated ALG hydrogel particles was also reported in microencapsulated *Bifidobacterium longum* [40]. Among all chitosan coated particles, the secondary layer formed by COS presented the smoothest surface, followed by LMW–chitosan. The MMW–chitosan formed the roughest surface on the hydrogel particle. This was consistent with ζ–potential of the chitosan solutions with different MW. As the molecular weight of chitosan increased, stronger electrostatic interaction was anticipated between ALG and chitosan, giving rise to the higher portion of the secondary layer to be protruded to the surface of the hydrogel particles. In consequence, the surface of the hydrogel particles became more tanglesome. Similar results were also reported that the smaller molecular weight of chitosan used, the more uniform coating on particle surface were formed due to its low viscosity [41].

The interior structure of the hydrogel particles (**Figure 3 A-3, B-3, C-3 & D-3)** was porous which was a result of the ionic bridges formed between the G blocks on the backbone of sodium alginate and Ca^{2+} [42]. This "egg–box" model that illustrated the ionotropic gelation between alginate and $CaCl_2$ has been well demonstrated [43]. Overall the hydrogel particles coated with chitosan tended to have larger and more open cells inside than that of the control. Previous study also demonstrated that more amount of chitosan molecules attaching to the ALG hydrogel particles could break the "egg–box" model, resulting in a higher porosity of alginate core [44]. Interestingly, we observed that in **Figure 3 A-3**, the hydrogel particle maintained the porous property with visible rod-shaped LGG on the surface (the arrows in **Figure 3 A-2**). These characters were maintained to some levels in LMW–ALG particle in **Figure 3 B-3** and became invisible in **Figure 3 C-3& D-3**. It could be possible that the extruded part of the chitosan on the

surface of ALG–LMW and ALG–MMW particles blocked our sights from visualizing the pores. Therefore, no visible bacteria were observed on the surface. Still, further information is required to confirm this assumption.

FTIR spectra of freeze-dried hydrogel particles

In order to better understand whether and how MW of chitosan influenced the functional group interaction between chitosan solution and ALG hydrogel particles, the IR spectra of the four samples (ALG, ALG–COS, ALG–LMW, ALG–MMW) and the control (COS, LMW–chitosan and MMW–chitosan) were recorded in the range of 4000–750 cm^{-1} (**Figure 4**).

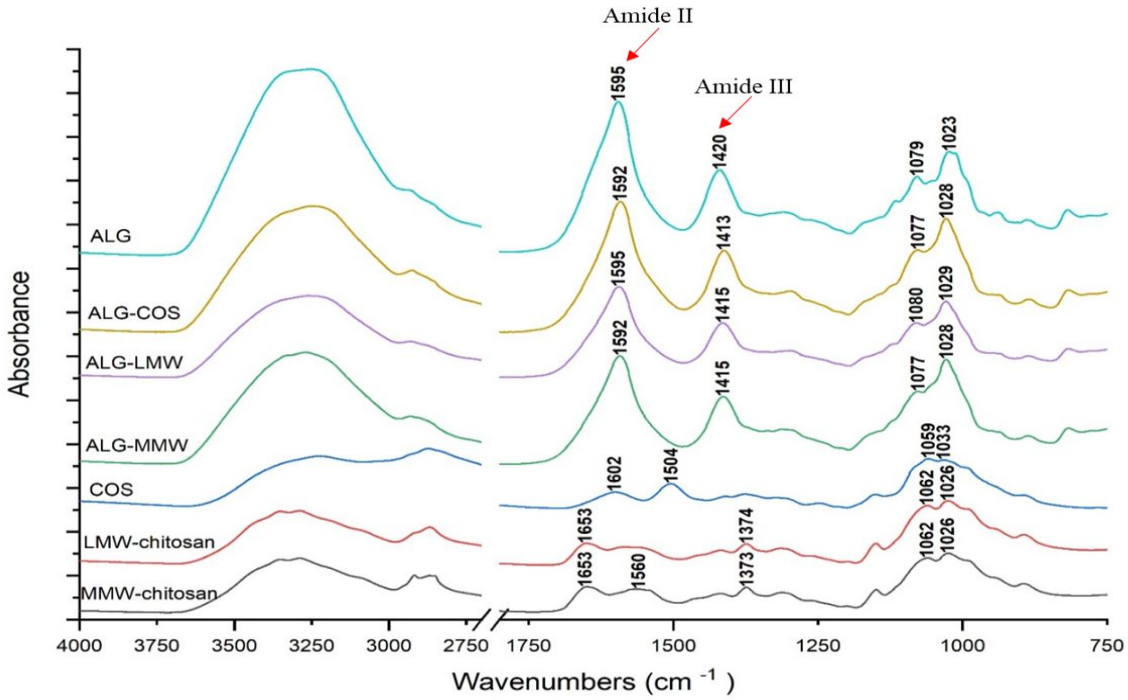

Fig 4. FTIR spectra of hydrogel particles in the absence and presence of chitosan coating (ALG, ALG–COS, ALG–LMW and ALG–MMW) and three kinds of chitosan (COS, LMW and MMW).

The three spectra presented on the bottom of **Figure 4** belonged to three types of chitosan. We could observe that the overall spectra of chitosan showed strong similarity except the slight differences on the signal strength. The band in the region 3290–3350 cm^{-1} was attributed to the N–H and O–H stretching, in conjunction with the intramolecular hydrogen bonds. The absorptions at 2875 and 2920 cm^{-1} corresponded to asymmetric and symmetric C–H stretching bands, respectively, which were widely reported in the spectra of other common polysaccharides, such as xylan [45] and carrageenan [46]. A similar absorption pattern around this region was observed in the spectrum of sodium alginate hydrogel particles, as shown on the top of **Figure 4**. The existence of residual N-acetyl groups in chitosan was confirmed by the bands at around 1653 cm^{-1} in the spectra of LMW and MMW chitosan and around 1602 cm^{-1} in the spectrum of COS (C=O stretching of amide I group), as well as the absorptions at 1560 cm^{-1} in the spectrum of MMW chitosan and 1504 cm^{-1} in the spectrum of COS (N–H bending of amide II group), respectively. The band at 1374 cm^{-1} was attributed to the $–CH_3$ symmetrical deformations. The bands at 1062 and 1026 cm^{-1} corresponded to C–O stretching, which were also present in the spectrum of ALG. These characteristics were consistent with the findings of others [47, 48]. With respect to the spectrum of ALG, except for the general bands mentioned above, the strong absorptions at both 1595 and 1420 cm^{-1} were registered to the asymmetric and symmetric stretching peaks of $–COO^–$, respectively [49].

The three spectra in the middle of **Figure 4** corresponded to the three types of chitosan coated ALG hydrogel particles. In general, all chitosan coated hydrogel particles showed slight shift in peaks of amide II, and III towards lower wavenumbers compared to ALG presumably due to the electrostatic interaction between the amino groups of chitosan (NH_3^+) and carboxylic groups of ALG ($–COO^–$). A similar wavenumber shift was also reported in chitosan coated

calcium-alginate nanocapsules [21]. Furthermore, wavenumber shifts occurred in the two peaks in "fingerprint region" (approximately 1020–1080 cm^{-1}) of chitosan coated particles. In short, the FTIR results demonstrated that chitosan with different molecular weight had similar IR spectrum and that all of them were attached to the surface of sodium alginate hydrogel particles through electrostatic interaction.

Textural properties of the hydrogel particles

Previous studies suggested that the texture properties and functional performance (e.g., viability of probiotics, control and release) of probiotics encapsulated by hydrogel particles were largely determined by the coating and/or wall material composition and concentration [50, 51]. For example, it has been reported that there is a correlation between storage stability of probiotics encapsulated in hydrogel particles and hardness of hydrogel particles [20]. Consequently, the textural properties of hydrogel particles were measured and presented in **Table 1**.

Among all the samples, ALG–COS showed a significantly higher hardness and springiness. It also required more force to be ruptured compared to the others but had comparable cohesiveness and resilience ($p > 0.05$). This was expected since smaller MW of COS can form a homogeneous, intact and rigid layer outside of the ALG hydrogel particles as corroborated by the morphological study (**Figure 3 B-2**). Besides, the hardness of particles decreased as the increase of chitosan MW. For instance, MMW chitosan coated ALG particles had the lowest hardness among all the tested hydrogel particles ($p < 0.05$), which can be explained by the relatively looser interaction between alginate and MMW chitosan on the surface of particles which promoted the decrease of the internal Ca^{2+} cross–linking between alginate and Ca^{2+} as indicated by cross-section morphology of particles (**Figure 3 D-2**).

Table 1. Textural properties of hydrogel particles with and without chitosan coating.

	Hardness (g)	Rupture force (g)	Springiness	Cohesiveness	Resilience
ALG	359.60 ± 18.50 [b]	126.45 ± 9.60 [b]	1.86 ± 0.01 [b]	8.25 ± 1.52 [a]	0.42 ± 0.00 [a]
ALG-COS	426.98 ± 10.00 [a]	151.08 ± 5.24 [a]	2.01 ± 0.00 [a]	8.19 ± 0.23 [a]	0.44 ± 0.02 [a]
ALG-LMW	306.40 ± 17.70 [c]	128.03 ± 6.15 [ab]	1.88 ± 0.04 [b]	6.91 ± 0.35 [a]	0.45 ± 0.01 [a]
ALG-MMW	266.45 ± 1.71 [d]	126.29 ± 12.34 [b]	1.91 ± 0.04 [b]	6.57 ± 0.40 [a]	0.46 ± 0.01 [a]

Different lowercase superscripts indicate that the intraspecific means differ significantly (p <0.05).

Viability of capsulated LGG during long-term storage

One of major challenges to retard the application of probiotics in the food industry is the viability loss during product storage period. Commercial probiotics fortified products may undergo different storage temperatures such as stored in the refrigerator or at an ambient condition. As such, the impact of chitosan on the viability of encapsulated LGG in hydrogel particles at different storage temperature (i.e., 37, 25 and 4 °C) were shown in **Figure 5**. Under 37 °C storage, a significant loss of viability (≈6 log CFU/g) was observed after 7 days of storage in all samples except for ALG–COS, in which the viability loss was around 5 log CFU (**Figure 5A**). After 7 days storage, the inactivation rate of the cells slowed down and stayed relatively stable till 30 days of storage. Therefore, we concluded that the majority loss of cell viability occurred in the first week and after then, the survived bacteria tended to stay activate in the hydrogel particles until 30 days when stored at 37 °C. Among all the hydrogel particles, ALG–COS showed a better protection on the viability of encapsulated LGG over the entire course of storage time. **Figure 5B** showed the viability of encapsulated LGG in hydrogel particles during 90 days of storage at 25 °C. In general, the viability loss rate of LGG was high at the beginning (approximately 13 days), which were then entered into a relatively stable phase (13–50 days),

and followed by a gradual decrease afterwards. An apparently higher viable cell count was observed in ALG–COS during storage and it was determined as 4.88 log CFU/g after 90 days of storage. Concerning the other three samples, the counts of viable cells were roughly identical during the whole storage period, which indicated that LMW–chitosan and MMW–chitosan showed no improvement on the viability of encapsulated LGG. In light of the reduction of viable cells over storage time, it can be deduced that the majority of loss appeared in the first several days.

Being different from the higher storage temperature, the viability loss rate of LGG encapsulated in all hydrogel particles was gradually decreased when stored at 4 °C, as shown in **Figure 5C**. After 90 days of storage, the viable cell count was maintained around 5 log CFU/g in all samples. This was not a surprise since 4 °C is a recommended storage condition for bacteria. These results demonstrated that storage temperature played an important role on the viability of probiotics in hydrogel particles. As we expected, the lower storage temperature rendered the higher shelf life of LGG. An increased storage stability in hydrogel particles was also found after they were coated with chitosan [20]. Additionally, we also found ALG coated with COS greatly improved the viability of encapsulated LGG during higher storage temperature (both 37 °C and 25 °C). One possible reason is that the penetration of molecular oxygen was largely retarded by homogeneously distributed COS layer outside of ALG hydrogel particles, which was proved by the textural analyzing and SEM results. A number of studies have shown that the oxygen content are the most important factors determining the viability of probiotics during the storage period [52]. Moreover, the prebiotic property of COS, as some previous studies reported [31, 32, 53], may also account for its ability to stimulate the growth of LGG, and hence reducing the viability loss during storage.

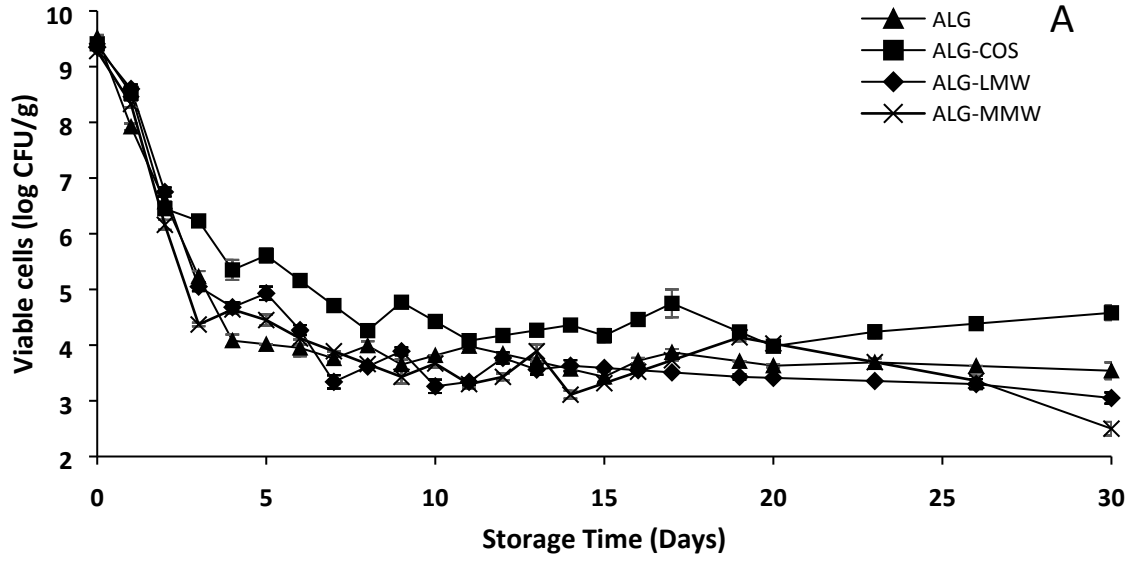
A
ALG
ALG-COS
ALG-LMW
ALG-MMW
Viable cells (log CFU/g)
Storage Time (Days)
10
9
8
7
6
5
4
3
2
0
5
10
15
20
25
30

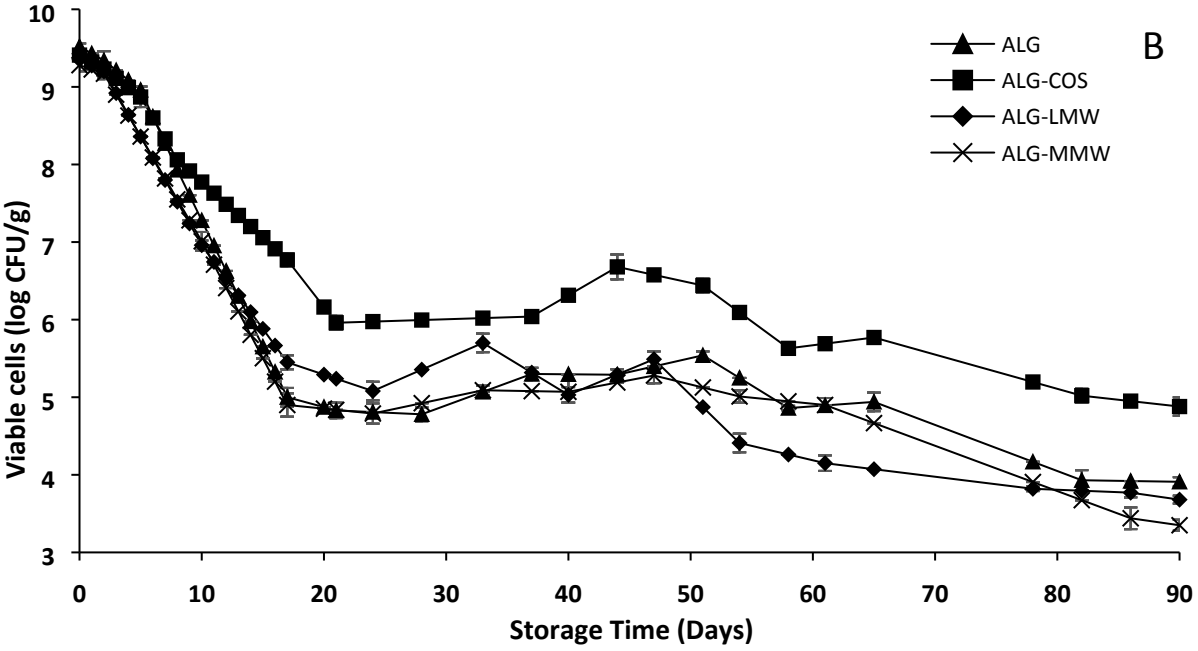
B
ALG
ALG-COS
ALG-LMW
ALG-MMW
Viable cells (log CFU/g)
Storage Time (Days)
10
9
8
7
6
5
4
3
0
10
20
30
40
50
60
70
80
90

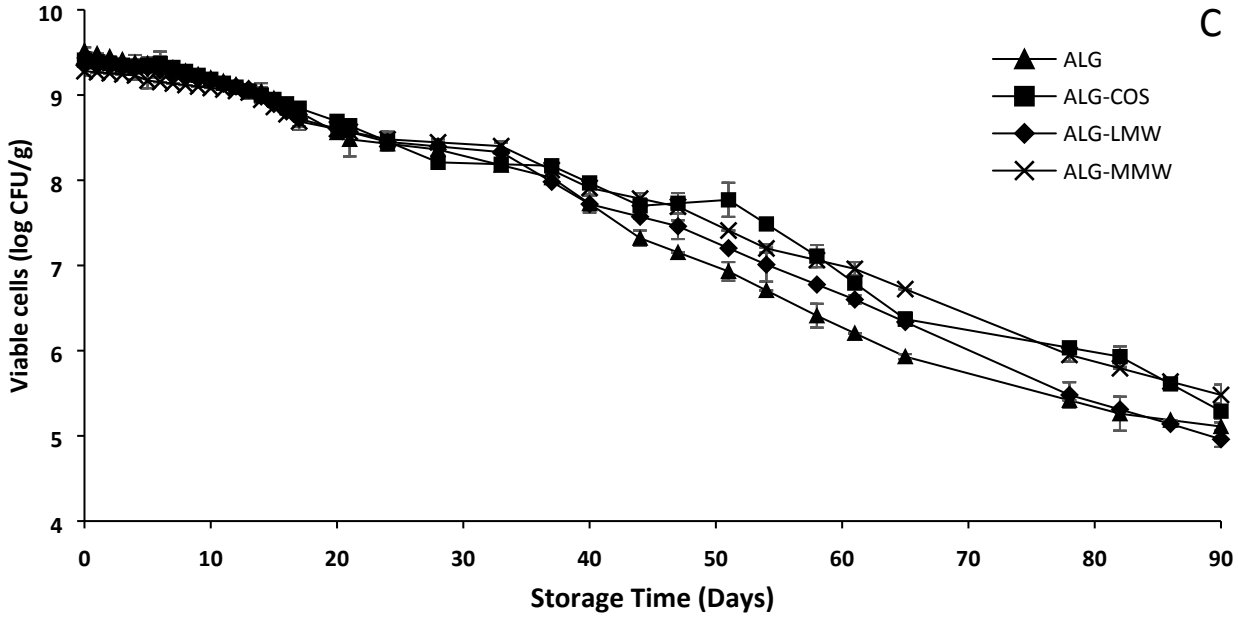

Fig. 5. Viable cells of LGG encapsulated in hydrogel particles in the presence and absence of chitosan coating during storage at (A) 37°C; (B) 25 °C and (C) 4°C.

Survival of encapsulated LGG in simulated gastrointestinal digestion

As we stated earlier, probiotics have to survive in our GI tract in large quantities to carry out positive health effects. Many previous studies have revealed that free LGG cells suffer a severe, even completely viability loss in SGF in a short *in vitro* digestion period [9, 54, 55]. Thus, we investigated the possible protective effects of secondary layer of chitosan with different MW on the viability of encapsulated LGG in simulated gastrointestinal conditions. The hydrogel particles coated in the absence and presence of different chitosan were incubated in SGF for 30, 60, 90 and 120 min and in SIF for 150 min. The viable counts of LGG at different time points were presented in **Figure 6**.

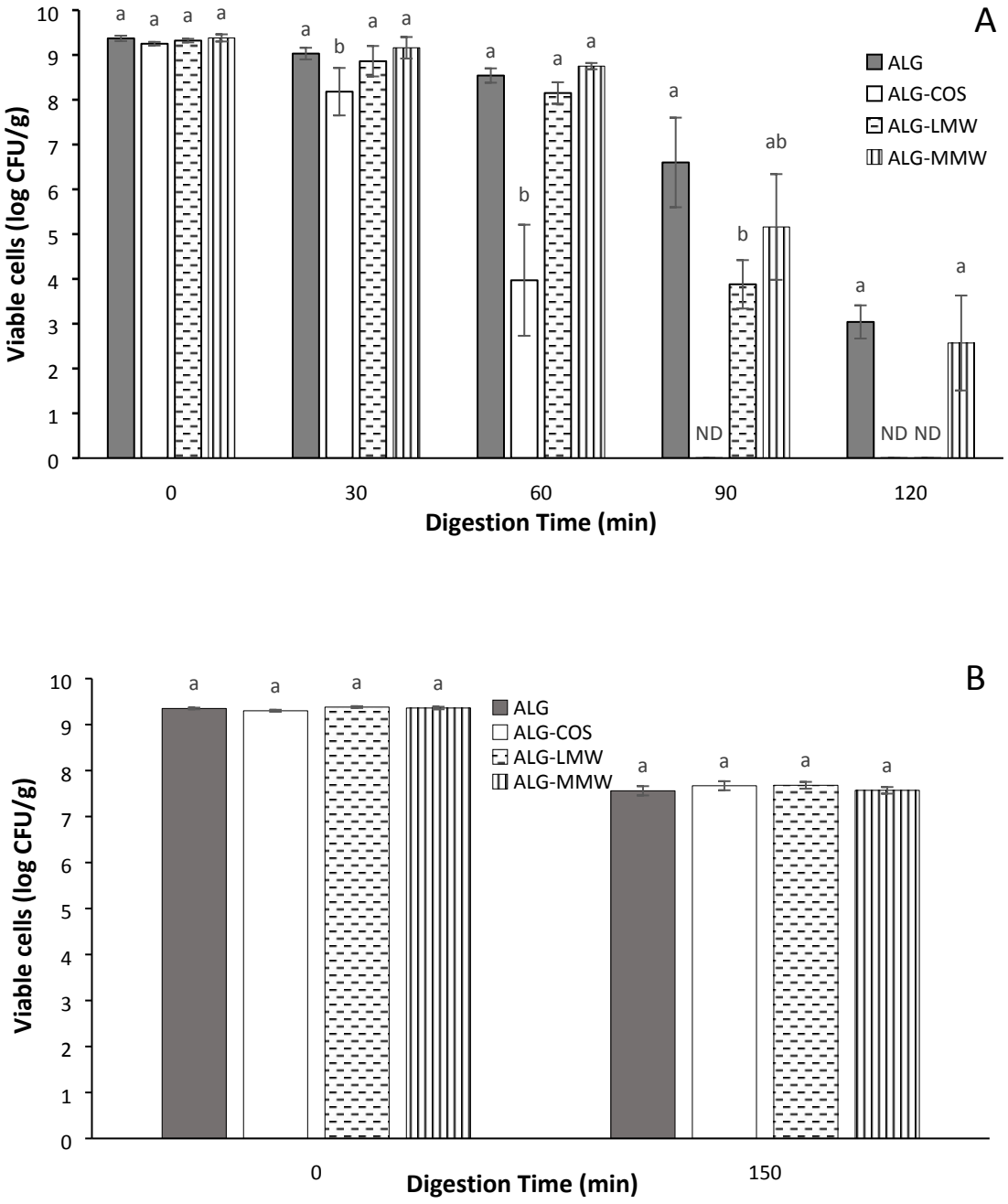

Fig 6. Viable cells count of LGG encapsulated in hydrogel particles in the absence and presence of chitosan coating after incubated (A) in simulated gastric fluid (SGF) at 0, 30, 60, 90, 120 min, (B) in simulated intestinal fluid (SIF) at 0 and 150 min. Different lowercase letters at same time point means differ significantly (p <0.05). ND: not detectable.

Figure 6A showed the viability of encapsulated LGG in SGF. In general, the viable cell counts of 9.4 log CFU/g in fresh hydrogel particles were achieved, and no significant difference was found between four samples. At the end of SGF stage (120 min), cell viability underwent at least a 6-log reduction. The possible explanation for this result was that the hydrogel particles produced in this method had relatively large pore size which facilitated the diffusion of small molecules, such as organic acids, oxygen and digestive enzymes into the hydrogel, hence deactivating the encapsulated LGG [56]. In terms of the three different chitosan, a slight reduction (~ 1 log CFU/g) was observed in all three treatments after 60 min digestion. The number of viable cells in ALG–COS, however, showed a drastic reduction (5.28 log CFU/g) with increasing incubation time and no viable cells could even be detected after 90 min incubation. Similarly, the viable cells in ALG–LMW became undetectable after 120 min digestion in SGF. Among the three hydrogel particles that coated with chitosan, ALG–MMW showed an apparently better protection on the survival of encapsulated LGG. One possible reason could be due to the highest swelling capacity of ALG upon coated by COS, as indicated by springiness value from texture analyzer. Such capacity could potentially decrease the cross-linking density of the ALG, which allowed a larger amount of gastric fluid to penetrate into the hydrogel. In addition, COS is highly soluble at acidic pH, which also favored gastric fluid reflux. This result was in line with previously report [41], where the survival rate of *Lactobacillus bulgaricus* KFRI 673 was enhanced in higher molecular weight of chitosan coated alginate particles than that of low molecular weight of chitosan. Similar survival rate of probiotics encapsulated in multilayer chitosan coated alginate particles under SGF solution were also documented [57]. Interestingly, we found that viable cells of LGG encapsulated in ALG and ALG–MMW remained on a comparable level which was 3.04 and 2.57 log CFU/g, respectively, after 120 min digestion in SGF. Apparently,

there was no survival rate improvement in encapsulation of LGG in chitosan-coated alginate compared with cells in ALG particles. In fact, mixed results on the probiotics survival rate were reported when they were encapsulated in alginate and chitosan hydrogel particles. For instance, some studies found the similar results as presented here and postulated that modified surface charge of alginate hydrogel by MMW chitosan did not improve viability of the selected *bifidobacterial* cells during simulated digestion [40]. Many others found that the survival rate of probiotics, such as encapsulated *lactobacilli* in ALG coated with chitosan was greater than it in ALG in SGF condition [58]. Such discrepancy may be attributed to the differences on the probiotics applied, the concentrations of alginate and chitosan, and the formation of hydrogel conditions. For instance, the survival rate of encapsulated probiotics in SGF was strongly dependent on the concentration of the alginate and chitosan as well as other external factors such as the concentration of the gelling solution [36, 59].

Fig. 6B displayed the viable cells count in hydrogel particles in the absence/ presence of chitosan coating before and after incubation in SIF for 150 min. The viability losses of encapsulated LGG in all hydrogel particles during SIF digestion were in the range from 1.63 to 1.79 log CFU/g; however, there was also no statistically significant difference among them ($p > 0.05$), indicating the four treatments were identical in probiotic protection under SIF condition. The different performances of hydrogel particles on protecting the encapsulated LGG under SGF and SIF conditions manifested that the main challenge in exerting the protective effect on probiotics viability is to prevent the diffusion of H^+ from SGF into the hydrogel particles.

Conclusions

There is a challenge on the survival rate of probiotics during long-term storage and when traveling through human GI tract. Microencapsulation based delivery systems such as chitosan

coated sodium alginate hydrogel particles have been applied for improving the viability of probiotics. However, the role of chitosan molecular weight for the encapsulation and protection of probiotics has yet to be systematically developed. In this work, we carried out an extensive study on how the secondary layer of three types of chitosan influenced the physicochemical properties of the sodium alginate hydrogels and the viability of the encapsulated LGG during storage period and simulated GI tract.

Successfully deposition of three type of chitosan (COS, LMW–chitosan, MMW–chitosan) on sodium alginate hydrogel particles was proved by the FTIR spectrum and SEM images. In terms of the impact of chitosan MW on the storage stability of probiotics, probiotics encapsulated in COS coated sodium hydrogel particles exhibited the highest survival rate during storage at all three temperature (4, 25, and 37). This is because of the uniform and denser surface as well as and the greater hardness and rupture force delivered by the COS coating deposited on hydrogel particles that prevent molecular oxygen from diffusion in hydrogel particle. However, we found all three secondary layer of chitosan had no effect on improving the viability of encapsulated LGG in stomach fluid compared to sodium alginate hydrogel particles. We believed that our research could help with understanding the roles of secondary chitosan layer on alginate hydrogel particles in improving the storage stability. It could also provide insights on searching materials that can help probiotics tolerate harsh H^+ in stomach.

Conflict of Interest

There are no conflicts to declare.

Acknowledgements

This work is partially supported by USDA National Institute of Food and Agriculture (Hatch ND1594) and ND EPSCoR Research Seed Award (FAR0032229). We also thank Kristin Whitney at NDSU for her assistance on texture analysis experiment.

References

1. M. H. Saier and N. M. Mansour, *Journal of Molecular Microbiology and Biotechnology*, 2005, **10**, 22-25.
2. T. Mach, *Journal of Physiology and Pharmacology*, 2006, **57**, 23-33.
3. A. C. Ouwehand and S. J. Salminen, *International Dairy Journal*, 1998, **8**, 749-758.
4. H. Liu, J. Gong, D. Chabot, S. S. Miller, S. W. Cui, F. Zhong and Q. Wang, *Food Hydrocolloids*, 2018, **78**, 100-108.
5. N. P. Shah, W. E. V. Lankaputhra, M. L. Britz and W. S. A. Kyle, *International Dairy Journal*, 1995, **5**, 515-521.
6. K. M. Amine, C. P. Champagne, Y. Raymond, D. St-Gelais, M. Britten, P. Fustier, S. Salmieri and M. Lacroix, *Food Control*, 2014, **37**, 193-199.
7. M. Saarela, I. Virkajärvi, H.-L. Alakomi, P. Sigvart-Mattila and J. Mättö, *International Dairy Journal*, 2006, **16**, 1477-1482.
8. J. Laličić-Petronijević, J. Popov-Raljić, D. Obradović, Z. Radulović, D. Paunović, M. Petrušić and L. Pezo, *Journal of Functional Foods*, 2015, **15**, 541-550.
9. J. Burgain, C. Gaiani, C. Cailliez-Grimal, C. Jeandel and J. Scher, *Innovative Food Science & Emerging Technologies*, 2013, **19**, 233-242.
10. S. S. Pinto, C. B. Fritzen-Freire, S. Benedetti, F. S. Murakami, J. C. C. Petrus, E. S. Prudêncio and R. D. M. C. Amboni, *Food Research International*, 2015, **67**, 400-408.

11. M. T. Cook, G. Tzortzis, D. Charalampopoulos and V. V. Khutoryanskiy, *Journal of Controlled Release*, 2012, **162**, 56-67.

12. M. J. Martin, F. Lara-Villoslada, M. A. Ruiz and M. E. Morales, *Innovative Food Science & Emerging Technologies*, 2015, **27**, 15-25.

13. W. Krasaekoopt, B. Bhandari and H. Deeth, *International Dairy Journal*, 2003, **13**, 3-13.

14. J. Burgain, C. Gaiani, M. Linder and J. Scher, *Journal of Food Engineering*, 2011, **104**, 467-483.

15. Q.-Y. Dong, M.-Y. Chen, Y. Xin, X.-Y. Qin, Z. Cheng, L.-E. Shi and Z.-X. Tang, 2013, **48**, 1339-1351.

16. A. K. Anal and H. Singh, *Trends in Food Science & Technology*, 2007, **18**, 240-251.

17. P. de Vos, M. M. Faas, M. Spasojevic and J. Sikkema, *International Dairy Journal*, 2010, **20**, 292-302.

18. B. L. Strand, Y. A. Morch and G. Skjak-Braek, *Minerva Biotechnologica.*, 2000, **12**, 223-233.

19. A. R. Donthidi, R. F. Tester and K. E. Aidoo, *Journal of Microencapsulation*, 2010, **27**, 67-77.

20. S. Nualkaekul, D. Lenton, M. T. Cook, V. V. Khutoryanskiy and D. Charalampopoulos, *Carbohydrate Polymers*, 2012, **90**, 1281-1287.

21. F. Shamekhi, E. Tamjid and K. Khajeh, *International Journal of Biological Macromolecules*, 2018, **120**, 460-467.

22. D. W. Lee, C. Lim, J. N. Israelachvili and D. S. Hwang, *Langmuir*, 2013, **29**, 14222-14229.

23. Y. Zhou, E. Martins, A. Groboillot, C. P. Champagne and P. C. Neufeld, *Journal Applied Microbiology*, 1998, **84**, 342-348.

24. I. Trabelsi, W. Bejar, D. Ayadi, H. Chouayekh, R. Kammoun, S. Bejar and R. B Salah, *International Journal of Biological Macromolecules*, 2013, **61**, 36-42.

25. M. Bourne, *Food Texture and Viscosity: Concept and Measurement*, Elsevier, 2002.

26. O. Sandoval-Castilla, C. Lobato-Calleros, H. S. García-Galindo, J. Alvarez-Ramírez and E. J. Vernon-Carter, *Food Research International*, 2010, **43**, 111-117.

27. Y. Lan, M. Xu, J.-B. Ohm, B. Chen and J. Rao, *Food Chemistry*, 2019, **278**, 665-673.

28. A. V. Rao, N. Shiwnarain and I. Maharaj, *Canadian Institute of Food Science and Technology Journal*, 1989, **22**, 345-349.

29. M. Xu, F. Gagné-Bourque, M.-J. Dumont and S. Jabaji, *Journal of Food Engineering*, 2016, **168**, 52-59.

30. Y. Wang, A. Khan, Y. Liu, J. Feng, L. Dai, G. Wang, N. Alam, L. Tong and Y. Ni, *Carbohydrate Polymers*, 2019, **223**, 115061.

31. C. Muanprasat and V. Chatsudthipong, *Pharmacology & Therapeutics*, 2017, **170**, 80-97.

32. H.-W. Lee, Y.-S. Park, J.-S. Jung and W.-S. Shin, *Anaerobe*, 2002, **8**, 319-324.

33. R. S. Rabelo, I. F. Oliveira, V. M. da Silva, A. S. Prata and M. D. Hubinger, *International Journal of Biological Macromolecules*, 2018, **119**, 902-912.

34. Q. Luo, J. Zhao, X. Zhang and W. Pan, *International Journal of Pharmaceutics*, 2011, **403**, 185-191.

35. A. Einbu, H. Grasdalen and K. M. Vårum, *Carbohydrate Research*, 2007, **342**, 1055-1062.

36. P. E. Ramos, P. Silva, M. M. Alario, L. M. Pastrana, J. A. Teixeira, M. A. Cerqueira and A. A. Vicente, *Food Hydrocolloids*, 2018, **77**, 8-16.

37. P. Muthukumarasamy, P. Allan-Wojtas and R. A. Holley, *Journal of Food Science*, 2006, **71**, M20-M24.

38. S. M. Koo, Y. H. Cho, C. S. Huh, Y. J. Baek and J. Park, *Journal of Microbiology and Biotechnology.*, 2001, **11**, 376-383.

39. Q. Zhao, A. Mutukumira, S. J. Lee, I. Maddox and Q. Shu, *World Journal of Microbiology and Biotechnology*, 2012, **28**, 61-70.

40. T. W. Yeung, E. F. Ucok, K. A. Tiani, D. J. McClements and D. A. Sela, *Frontiers in Microbiology*, 2016, **7**, 494.

41. J. Lee, D. Cha, and H. Park, *Journal of Agricultural and Food Chemistry*, 2004, **52**, 7300-7305.

42. O. Smidsrød and G. Skjak-Braek, *Trends in Biotechnology*, 1990, **8**, 71-78.

43. B. T. Stokke, K. I. Draget, O. Smidsrød, Y. Yuguchi, H. Urakawa and K. Kajiwara, *Macromolecules*, 2000, **33**, 1853-1863.

44. P. Sabitha, J. V. Ranta and K. R. Reddy, *International Journal of Chem Tech Research,* 2010, **2**, 88-98.

45. R. F. Melo-Silveira, G. P. Fidelis, M. S. S. P. Costa, C. B. S. Telles, N. Dantas-Santos, S. de O. Elias, V. B. Ribeiro, A. L. Barth, A. J. Macedo, E. L. Leite and H. A. O. Rocha, *International Journal of Molecular Sciences*, 2012, **13**.

46. F. R. F. Silva, C. M. P. G. Dore, C. T. Marques, M. S. Nascimento, N. M. B. Benevides, H. A. O. Rocha, S. F. Chavante and E. L. Leite, *Carbohydrate Polymers*, 2010, **79**, 26-33.

47. A. B. Vino, P. Ramasamy, V. Shanmugam and A. Shanmugam, *Asian Pacific Journal of Tropical Biomedicine*, 2012, **2**, S334-S341.

48. C. Song, H. Yu, M. Zhang, Y. Yang and G. Zhang, *International Journal of Biological Macromolecules*, 2013, **60**, 347-354.

49. B. Smitha, S. Sridhar and A. A. Khan, *European Polymer Journal*, 2005, **41**, 1859-1866.

50. A. Belščak-Cvitanović, D. Komes, S. Karlović, S. Djaković, I. Špoljarić, G. Mršić and D. Ježek, *Food Chemistry*, 2015, **167**, 378-386.

51. O. Sandoval-Castilla, C. Lobato-Calleros, H. García-Galindo, J. Alvarez-Ramírez and E. J. F. R. I. Vernon-Carter, *Food Research International*, 2010, **43**, 111-117.

52. M. K. Tripathi and S. K. Giri, *Journal of Functional Foods*, 2014, **9**, 225-241.

53. S. I. Mussatto and I. M. Mancilha, *Carbohydrate Polymers*, 2007, **68**, 587-597.

54. S. B. Doherty, M. A. Auty, C. Stanton, R. P. Ross, G. F. Fitzgerald and A. Brodkorb, *International Dairy Journal*, 2012, **22**, 31-43.

55. R. Li, Y. Zhang, D. B. Polk, P. M. Tomasula, F. Yan and L. Liu, *Journal of Controlled Release*, 2016, **230**, 79-87.

56. D. J. McClements, *Advances in Colloid and Interface Science*, 2015, **219**, 27-53.

57. M. T. Cook, G. Tzortzis, V. V. Khutoryanskiy and D. Charalampopoulos, *Journal of materials chemistry,* 2013, **1**, 52-60.

58. A. García-Ceja, E. Mani-López, E. Palou and A. López-Malo, *LWT - Food Science and Technology*, 2015, **63**, 482-489.

59. S. Abbaszadeh, H. Gandomi, A. Misaghi, S. Bokaei, N. Noori, *Journal of Science of and Food and Agriculture*, 2014, **94**, 2210-2216.

Graphical abstract

Chitosan coating improves the long-term stability of sodium alginate hydrogel particle but not the viability of probiotics it encapsulated